Four Acyltransferases Uniquely Contribute to Phospholipid Heterogeneity in *Saccharomyces cerevisiae*

Peter Oelkers[1] and Keshav Pokhrel[2]

[1]Department of Natural Sciences, University of Michigan–Dearborn, Dearborn, MI, USA. [2]Department of Mathematics and Statistics, University of Michigan–Dearborn, Dearborn, MI, USA.

ABSTRACT: Diverse acyl-CoA species and acyltransferase isoenzymes are components of a complex system that synthesizes glycerophospholipids and triacylglycerols. *Saccharomyces cerevisiae* has four main acyl-CoA species, two main glycerol-3-phosphate 1-*O*-acyltransferases (Gat1p, Gat2p), and two main 1-acylglycerol-3-phosphate *O*-acyltransferases (Lpt1p, Slc1p). The in vivo contribution of these isoenzymes to phospholipid heterogeneity was determined using haploids with compound mutations: *gat1Δlpt1Δ*, *gat2Δlpt1Δ*, *gat1Δslc1Δ*, and *gat2Δslc1Δ*. All mutations mildly reduced [3H]palmitic acid incorporation into phospholipids relative to triacylglycerol. Electrospray ionization tandem mass spectrometry identified few differences from wild type in *gat1Δlpt1Δ*, dramatic differences in *gat2Δslc1Δ*, and intermediate changes in *gat2Δlpt1Δ* and *gat1Δslc1Δ*. Yeast expressing Gat1p and Lpt1p had phospholipids enriched with acyl chains that were unsaturated, 18 carbons long, and paired for length. These alterations prevented growth at 18.5°C and in 10% ethanol. Therefore, Gat2p and Slc1p dictate phospholipid acyl chain composition in rich media at 30°C. Slc1p selectively pairs acyl chains of different lengths.

KEYWORDS: 1-acylglycerol-3-phosphate *O*-acyltransferase (AGPAT, LPAT), glycerol-3-phosphate 1-*O*-acyltransferase (GPAT), lipidomics, membranes, tandem mass spectrometry

Introduction

Fatty acids and the corresponding acyl chains may vary with respect to length, number, and position of double bonds and branches. The allocation of these species during the synthesis and remodeling of glycerophospholipids (PL), along with head group modification, determines the array of cellular PL species. Cellular PL composition influences membrane structure and dynamics, which affects cellular functions including vesicle fusion,[1,2] lateral migration of membrane proteins,[3] membrane protein orientation,[4] and passive diffusion of hydrophobic solutes.[5] Specific PL species can also bind receptors. For example, 1-palmitoyl-2-oleoyl-sn-glycerol-3-phosphocholine activates the mouse peroxisomal proliferator-activated receptor α and 1,2-diacyl-sn-glycero-3-phosphate (PA) with two saturated acyl chains binds and sequesters the fungal transcriptional repressor, Opi1p.[6,7]

Saccharomyces cerevisiae provides a relatively simple model system to understand acyl chain allocation. There is only one acyl-CoA desaturase, Ole1p, which can introduce a double bond at position Δ9.[8] Most acyl chains have 16 or 18 carbons.[9] Numerous studies utilizing electrospray ionization tandem mass spectrometry (ESI-MS[2]) have established that the four main acyl chains are not homogenously distributed among the approximately 80 detectable PL species.[10–17] In common laboratory conditions, yeast preferentially place saturated acyl chains in the sn-1 position.[9] Saturated acyl chains are also differentially distributed among PL head group species. In yeast cultured in rich media at 24°C, 53%, 29%, and 15% of acyl chains in 1,2-diacyl-sn-glycero-3-phospho-(1′-myo-inositol) (PI), 1,2-diacyl-sn-glycero-3-phosphoserine (PS), and 1,2-diacyl-sn-glycero-3-phosphocholine (PC), respectively, were saturated.[12] PC synthesized by methylation of 1,2-diacyl-sn-glycero-3-phosphoethanolamine (PE) almost exclusively contains unsaturated acyl chains while PC synthesized from CDP-choline has a mix of saturated and unsaturated chains.[11] The distinct asymmetry of acyl chain allocation supports that cellular mechanisms actively maintain PL homeostasis. The same mechanisms are likely responsible for changing PL composition in response to stimuli such as changing temperature and nutrient availability.[12,13,18] Acyltransferases with distinct substrate specificities are prime candidates for being components of these mechanisms.

As in other eukaryotes, acyl chain distribution in yeast is mediated in part by the two acyltransferases that initiate the synthesis of PL and triacylglycerol (TAG; Fig. 1). The first is acyl-CoA-dependent glycerol-3-phosphate 1-O-acyltransferase (GPAT, EC 2.3.1.15), which incorporates acyl chains into the sn-1 position of glycerol-3-phosphate or dihydroxyacetone phosphate. Two GPATs have been identified in *S. cerevisiae*: Gat1p (also named Gpt2p) and Gat2p (also named Sct1p) share 31% amino acid sequence identity.[19] Compound deletion of *GAT1* and *GAT2* is synthetically lethal,[19] indicating that these are the major if not only GPATs. To what extent the enzymes are redundant or specialized has not been unambiguously determined. This is due in part to kinetic parameters not being established for either. Deleting *GAT1* reduced in vitro GPAT activity by 88%, while deleting *GAT2* reduced activity by 35%. Overexpression of *GAT1* in a *gat1Δ* background showed similar in vitro GPAT activity with 65 μM of palmitoyl-CoA, palmitoleoyl-CoA, or oleoyl-CoA. Activity with stearoyl-CoA was 40% lower. Parallel analysis of *GAT2* yielded a continuum of activity with palmitoleoyl-CoA > palmitoyl-CoA > oleoyl-CoA > stearoyl-CoA.[19]

Gat1p may be specialized for incorporating unsaturated acyl-CoA into TAG. Culturing in media with 0.1% oleate limited the growth of *gat1Δ* but not *gat2Δ* strains.[20] Exposing Gat1p-GFP expressing yeast to 3.5 mM oleate resulted in fluorescence at crescent-shaped structures that seemed to connect lipid droplets with the endoplasmic reticulum. Gat2p-GFP did not associate with the crescents, and crescents were not observed with palmitate feeding.[21] However, *gat1Δ* strains incorporated 50% more [14C]acetate into TAG, while *gat2Δ* strains incorporated 50% less into TAG.[22]

Other evidence supports that Gat1p is specialized for incorporating unsaturated acyl chains into PL. Deletion of *GAT2* in a *pct1Δ* background, where PC synthesis is limited to the methylation of PE, reduced the abundance of PC with 34 acyl chain carbons and one double bond (PC 34:1) by 45% with a balanced increase in PC 34:2.[14] Overexpression of *GAT2* had the opposite effect, increasing monounsaturated PC species at the expense of diunsaturated PC species.[14,23] Whether these differences account for *gat1Δ* yeast having an elongated morphology compared to a round shape for *gat2Δ* yeast has not been determined.[24]

The lysoPA generated by GPAT may be esterified by acyl-CoA-dependent 1-acylglycerol-3-phosphate O-acyltransferase (AGPAT; EC 2.3.1.51) to make PA. In addition to being an intermediate in PL and TAG synthesis (Fig. 1), PA regulates transcription by sequestering the Opi1p transcription factor in the endoplasmic reticulum.[25] PA can also promote mitochondrial outer membrane synthesis.[26] Four AGPATs have been identified in *S. cerevisiae*: Slc1p,[27] Lpt1p (also named Ale1p, Slc4p, Lca1p),[15,28–32] Ict1p,[33] and Loa1p.[34] Compound deletion of *SLC1* and *LPT1*, which are not homologs, resulted in synthetic lethality,[28,31,32] supporting that these are the major AGPATs. As with the GPATs, whether Slc1p and Lpt1p are redundant or specialized is not completely understood.

Deletion of *SLC1* reduced in vitro AGPAT activity by 30%–50%.[28,30] Kinetic parameters have not been determined for Slc1p. Comparing AGPAT activity in wild-type and *slc1Δ* microsomes using 40 nM of various acyl-CoA species supported that Slc1p utilizes medium chain, saturated acyl-CoA species equally well as oleoyl-CoA.[35] However, supplying *lpt1Δ* microsomes with 50 μM oleoyl-CoA showed five-fold higher AGPAT activity than with 50 μM palmitoyl-CoA.[28] Purified GST-Slc1p esterified 50 μM lysoPA, lysoPI, and lysoPS with similar velocity.[15] Therefore, Slc1p may mediate some PL remodeling as well as de novo synthesis. Slc1p also esterified lysoPC and lysoPE, but to a much lesser extent.[15] Surprisingly, ESI-MS[2] analysis of PL species in *slc1Δ* and wild-type yeast grown in YP media with galactose at 30°C showed very similar profiles.[15]

Deletion of *LPT1* resulted in either a modest or a profound reduction of in vitro AGPAT activity.[28,29,32] Unambiguous is the profound reduction in lysoPC, lysoPE, lysoPI, and lysoPS esterification in *lpt1Δ* microsomes.[28,29,31,36] Kinetic analysis of lysoPC esterification upon *LPT1* overexpression found apparent V_{max} values for the unsaturated palmitoleoyl-CoA and oleoyl-CoA to be 10–15-fold higher than for the saturated palmitoyl-CoA and stearoyl-CoA species.[28,36] Apparent K_m values were 10-fold lower for the saturated species. Based on these parameters, if cellular acyl-CoA concentrations are above 10 μM, Lpt1p will preferentially incorporate unsaturated acyl chains. Whether this specificity varies among lysoPL species has not been determined. ESI-MS[2] analysis of *lpt1Δ* strains showed a modest shift from PL with 32 carbons in the acyl chains to those with
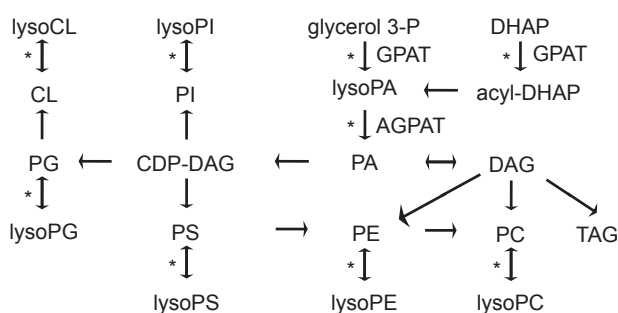
Figure 1. Schematic of phospholipid synthetic pathways in *S. cerevisiae*. Arrows indicate catalyzed reactions to form the indicated intermediates. Asterisks indicate acyl-CoA-dependent reactions. Not all substrates, intermediates (eg, glycerophosphocholine), and reactions (eg, phospholipid diacylglycerol acyltransferase) were shown for simplicity.

Abbreviations: AGPAT, 1-acylglycerol-3-phosphate O-acyltransferase; CDP-DAG, cytidine diphosphate-diacylglycerol; DAG, diacylglycerol; DHAP, dihydroxyacetone phosphate; GPAT, glycerol-3-phosphate 1-O-acyltransferase; PA, 1,2-diacyl-sn-glycero-3-phosphate; PC, 1,2-diacyl-sn-glycero-3-phosphocholine; PE, 1,2-diacyl-sn-glycero-3-phosphoethanolamine; PG, 1,2-diacyl-sn-glycero-3-phospho-(1′-sn-glycerol); PI, 1,2-diacyl-sn-glycero-3-phospho-(1′-myo-inositol); PS, 1,2-diacyl-sn-glycero-3-phosphoserine; TAG, triacylglycerol.

34 carbons.[15] Since Lpt1p and, to a lesser extent, Slc1p can esterify lysoPL besides lysoPA, their contribution to PL acyl chain distribution likely goes beyond de novo PA synthesis. In vivo pulse-chase with [14C]choline found *lpt1Δ* strains to reesterify about four times less glycerophosphocholine than wild type.[30] Deletion of *LPT1* slowed growth in medium containing dioctanoyl PC, suggesting reduced remodeling capability.[37] In *Candida albicans*, deletion of the *LPT1* homolog significantly slowed the remodeling that occurred after PL composition was skewed with palmitate feeding.[38]

Experiments that systematically measure the contributions of two GPATs and two AGPATs to acyl chain allocation in *S. cerevisiae* are described here. Comparisons among strains genetically limited to produce only one major isoenzyme of GPAT and one AGPAT offer an unprecedented opportunity to isolate the contribution of the respective enzymes in vivo.

Methods

Materials. Chemicals were mainly obtained from Sigma, Fisher, and Sunrise (yeast media). [9,10-3H(N)]palmitate (30.0 Ci/mmol) and [9,10-3H(N)]oleate (54.5 Ci/mmol) were from PerkinElmer.

Yeast strains and culturing. All *S. cerevisiae* strains were W303 haploids (*ade2-1, can1-1, trp1-1, ura3-1, his3-11, 15, leu2-3, 112*).[39] ODY512 (*MATa slc1Δ::URA3*) and ODY545 (*MATa lpt1Δ::URA3*) were described previously.[28] ODY606 (*MATα, gat2Δ::URA3*) and ODY609 (*MATα, gat1Δ::URA3*) were generated by transforming a normal, W303-1B, haploid with polymerase chain reaction (PCR)-derived products containing 50 bp of gene-specific sequence flanking the *Kluyveromyces lactis URA3* sequence.[40] Haploid strains with the four possible genotypes of one GPAT and one AGPAT gene deletion were generated by crossing ODY512 with ODY609 and ODY606 and ODY525 with ODY609 and ODY606, respectively. Sporulation of these heterozygous diploids and dissection of tetrads followed by genotyping PCR identified haploid compound deletion mutants. Table 1 lists the strains used in this study. Yeast were cultured in YPD (2% (w/v) peptone, 1% (w/v) yeast extract, 2% (w/v) glucose) at 30°C unless otherwise indicated.

Table 1. *S. cerevisiae* strains generated and used in this study.

STRAIN	GENOTYPE (IN W303 BACKGROUND)
ODY636, ODY639	*MATa gat2Δ::URA3 lpt1Δ::URA3*
ODY641	*MATα gat2Δ::URA3 lpt1Δ::URA3*
ODY642	*MATα gat1Δ::URA3 lpt1Δ::URA3*
ODY644, ODY647	*MATa gat1Δ::URA3 lpt1Δ::URA3*
ODY648, ODY659	*MATa normal*
ODY652	*MATα normal*
ODY650, ODY653	*MATa gat2Δ::URA3 slc1Δ::URA3*
ODY656, ODY660	*MATα gat1Δ::URA3 slc1Δ::URA3*
ODY661	*MATa gat1Δ::URA3 slc1Δ::URA3*

Pulse labeling with [3H]palmitic acid and [3H]oleic acid. For three strains per genotype (two for *gat2Δslc1Δ*), stationary-phase cells were diluted 1:2,000 into YPD and grown until OD_{660} = 0.3–0.8. A total of 4 mL of cells were incubated with 166 nM of [3H]palmitic acid (30.0 Ci/mmol) or 92 nM [3H]oleic acid (54.5 Ci/mmol) for 30 minutes with shaking. Cells were harvested by centrifugation and washed twice with 5 mL 0.5% (v/v) Tergitol and once with 5 mL dH_2O. Lipids were extracted from cell pellets, resolved by thin-layer chromatography, and quantified by scintillation counting as described previously.[41]

Electrospray ionization tandem mass spectrometry (ESI-MS²) analysis of cellular phospholipids. Stationary-phase cultures for three strains per genotype (two for *gat2Δslc1Δ*) were diluted 1:500 into YPD and cultured at 30°C into log phase (Abs_{660} = 0.40–0.82). Cells were rinsed with phosphate-buffered saline and treated with 75 μL of 3 mg/mL lyticase, 0.2 mg/mL cyanide, and 10% (v/v) glycerol for 15 minutes at 37°C. Lipids were extracted as described previously and stored at −80°C prior to ESI-MS² analysis.[38] The process was repeated on two separate days for six biological replicates. As described previously,[42] polar lipids were analyzed using ESI-MS² at the Kansas Lipidomics Research Center. Briefly, 0.4 mg of cellular lipids were combined with two internal standards of each major PL head group in 1 mL of chloroform/methanol/300 mM ammonium acetate in water (300:665:35). Spectra were generated in a range of positive ion modes in a triple quadrupole mass spectrometer. Assignment of PL species was by identification of head group and mass/charge ratio. Signal comparison to the two respective internal standards allowed quantification. Abundances are reported as percent of all polar lipids detected.

Statistical analysis of phospholipid composition data. The proportion (*P*) of PL abundance data was grouped using the number of double bonds, acyl chain length, or head groups. Prior to analysis, all composition data were transformed using a log ratio, logit = ln(*P*/(1 − *P*)), developed previously and used for PL composition recently.[38,43] A total of 600 univariate statistical tests were performed on logit transformed compositional values of 60 different lipid species groupings to determine significant differences between the wild-type and four mutant genotypes and among the four mutant genotypes. Statistical calculations were performed using the program R, version 3.2.1. Tukey's post hoc test for multiple testing was used with false discovery rate. There were 292 significant ($p < 0.01$) comparisons among the genotypes. Hierarchical clustering was performed using Ward's minimum variance to group the genotypes according to their PL composition regarding number of double bonds, acyl chain lengths, or head groups.[44]

Growth assessment. Two strains of each genotype were cultured in YPD into log phase and diluted in YPD to 1,000 cells/μL. Three, 10-fold serial dilutions and spotting 4 μL onto gridded, agar plates allowed 4,000, 400, 40, and 4 cells to be applied to sequential spots for each strain.

Cells were cultured until a gradation of growth was observed. Alternatively, doubling times of three strains of each genotype (two for *gat2Δslc1Δ*) were determined by diluting stationary-phase cultures 1:800 in 10 mL of YPD and culturing at 30°C into early log phase (Abs$_{660}$ = 0.2–0.3). Cell density, as Abs$_{660}$, was measured every 30–60 minutes for three hours. Doubling time = (Time$_{(2)}$ – Time$_{(1)}$)*log 2/log (Abs$_{660(2)}$/Abs$_{660(1)}$).

Results

The synthesis and remodeling of PL involves many reactions that transfer acyl chains onto the glycerol backbone, indicated by asterisks in Figure 1. One hypothesis is that during synthesis, GPAT and AGPAT isoenzymes differentially generate and partition pathway intermediates and thereby direct production of different end products, namely, PL species and TAG. Such partitioning may involve distinct pools of lysoPA, PA, diacylglycerol (DAG), or CDP-DAG. Another hypothesis is that complementary substrate specificities of the GPAT and AGPAT isoenzymes allow for these enzymes to generate the physiological distribution of acyl chains in PL. Since there are two main GPATs (Gat1p, Gat2p) and two main AGPATs (Slc1p, Lpt1p) in *S. cerevisiae*, we used yeast as an experimental system to test these hypotheses. Haploid yeast strains with the four possible genotypes resulting from the deletion of one GPAT and one AGPAT were generated (Table 1). Comparing how these strains allocate acyl chains should elucidate each enzyme's contribution.

Short-term in vivo allocation of [³H]palmitic and [³H]oleic acids. Partitioning of fatty acids between PL and TAG was examined by pulse labeling studies (Fig. 2). Wild-type and compound deletion mutant yeast were incubated for 30 minutes with trace amounts of saturated [³H]palmitic acid or unsaturated [³H]oleic acid. Previous work has shown that after exogenous fatty acids are transported, they are utilized by the acyl-CoA synthetases Faa1p and Faa4p.[45] The corresponding acyl-CoA species may be utilized by

acyltransferases in both de novo synthesis and remodeling of PL and TAG.[9] Presuming that PL are more frequently remodeled than TAG, there will be a bias toward the incorporation of radiolabel into PL, regardless of genotype.

All of the mutants allocated palmitic acid with a reduced preference for PL synthesis as evidenced by a reduction in the PL/TAG ratio (Fig. 2C). The effect was possibly less in *gat1Δlpt1Δ* since that genotype's reduction did not reach statistical significance. The contribution of Slc1p to palmitic acid allocation is particularly evident. DAG abundance was reduced in both mutants harboring an *slc1Δ* allele (Fig. 2A). This reduction was also observed with oleic acid labeling (Fig. 2B). Lpt1p acting as the lone AGPAT may mediate a slower rate of PA production and thus DAG production while the subsequent utilization of PA and DAG is unabated, causing reduced DAG levels. The *gat2Δslc1Δ* strains were unique in having a significant, 30% reduction in total incorporation of palmitic acid (data not shown). All of the mutants also had mild reductions in the ratio of oleic acid incorporated into PL and TAG but none reached significance (Fig. 2C). Since it has been shown previously that the majority of exogenously provided palmitic acid can be recovered as palmitoleic acid after a two minute incubation, the differences observed between palmitic and oleic acid labeling may be more subtle than [what] is physiological.[9]

Steady-state in vivo acyl chain allocation measured by mass spectrometry. To assess the ability of the compound deletion mutant strains to generate the PL heterogeneity present in wild-type yeast, strains were cultured in rich medium into log phase. Cellular lipid extracts then underwent PL species analysis by electrospray ionization tandem mass spectrometry (ESI-MS²). The data array (five genotypes, 118 PL species, *n* = 6) was analyzed to answer three questions. Is the distribution of saturated and unsaturated acyl chains among PL altered in one or more of the compound mutants? Is the distribution of acyl chains of different lengths among
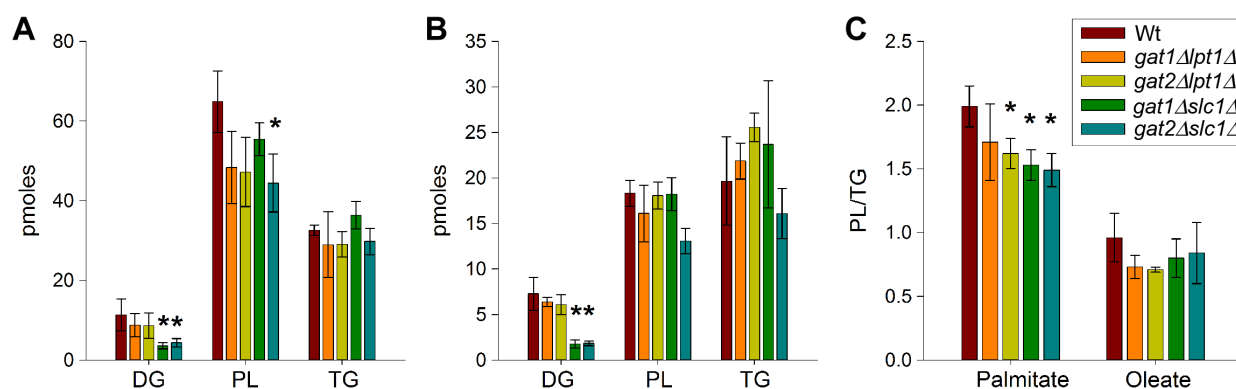
Figure 2. In vivo, pulse labeling with [³H]palmitic acid and [³H]oleic acid. Log-phase yeast cultures in YPD were incubated with 166 nM of [³H]palmitic acid or 92 nM of [³H]oleic acid for 30 minutes at 30°C. Cells were rinsed and lysed. Lipids were extracted, resolved by thin-layer chromatography, and quantified by liquid scintillation counting. (**A**) Moles of [³H]palmitic acid incorporated into DAG, TAG, and PL. (**B**) Moles of [³H]oleic acid incorporated into DAG, TAG, and PL (**C**) Ratio of incorporation into PL moles/TAG moles. *Indicates a statistically significant difference (*P* < 0.05) compared to wild type; *n* = 3; error bars are standard deviation.

PL altered in one or more of the compound mutants? Is the distribution of PL classified by head group altered in one or more of the compound mutants? The grouping of PL by these three criteria prior to analysis was guided by the hypothesis that acyl chain substrate specificity of the GPAT and AGPAT isoenzymes will guide PL composition during synthesis or remodeling. While comparing 60 lipid groupings among the genotypes provided for a comprehensive analysis, it also invoked a statistical penalty. Accordingly, subtle phenotypes may involve changes in abundance that did not reach statistical significance. Abundance of the individual PL species in each genotype is shown in Figure 3.
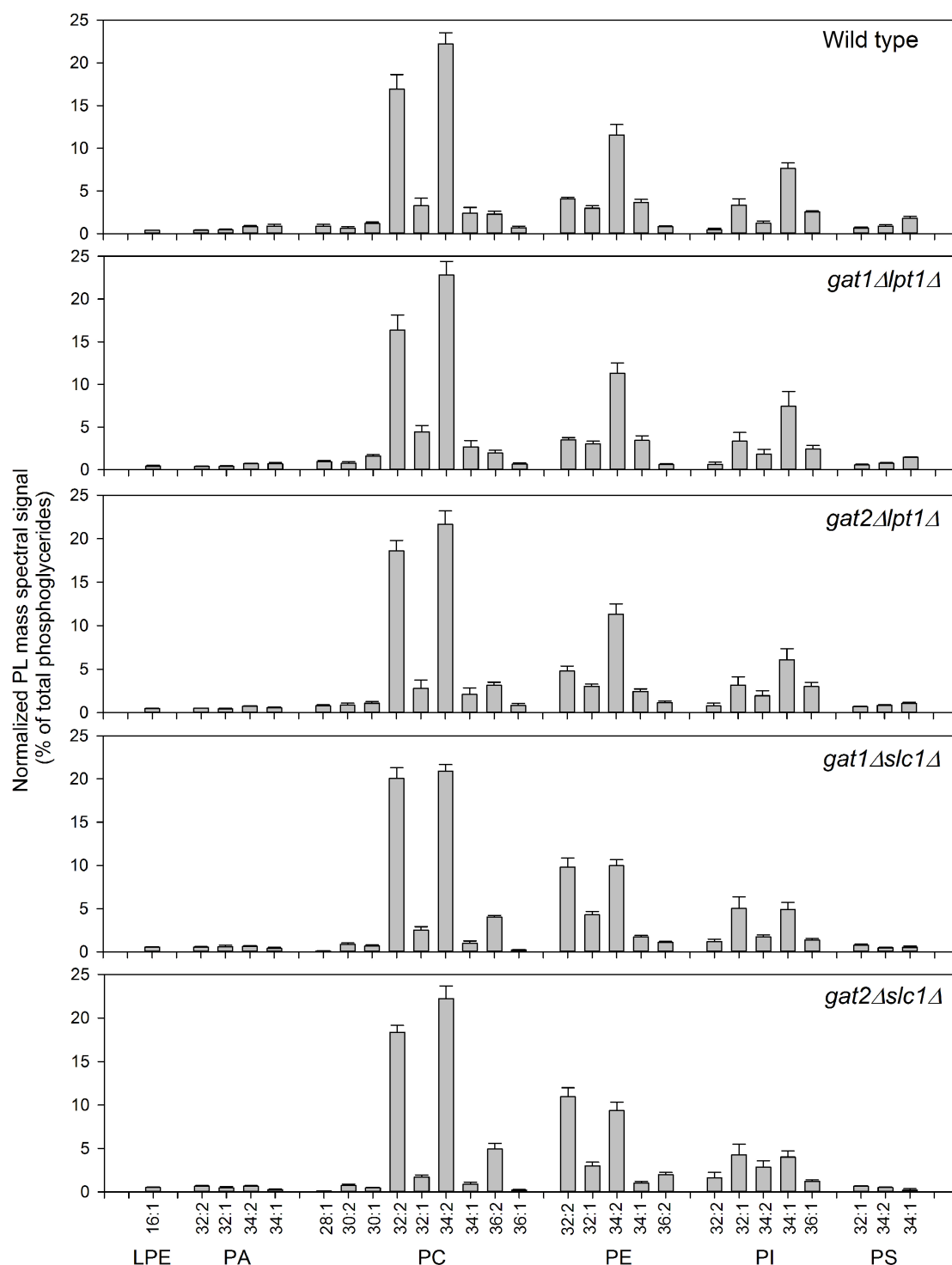
Figure 3. Composition of PL in wild-type and compound deletion mutant yeast. Three strains of each genotype (two for *gat2Δslc1Δ*) were grown in YPD at 30°C until log phase on two different days ($n = 6$). Extracted lipids were analyzed by ESI-MS^2 and the abundance of each species expressed as percent of total signal. Only species with an abundance >0.4% in wild-type strains are shown. Error bars are standard deviation.

Distribution of acyl chains in wild-type and mutant yeast: number of double bonds. When the PL compositions were categorized by number of double bonds in the acyl chains, a steady trend toward favoring unsaturated acyl chains was evident upon aligning the data from the wild type and four mutants in a heat map (Fig. 4B). The *gat1Δlpt1Δ* strains showed almost no differences compared to wild type. This is consistent with Gat2p and Slc1p mediating the majority of acyl chain distribution in wild-type cells in rich media at 30°C. When Gat1p was instead the main GPAT in *gat2Δlpt1Δ*, there was an increase in the abundance of all PL with two double bonds and a reduction in the proportion with one or zero. These changes are not statistically significant when compared to wild type but are significant when compared to *gat1Δlpt1Δ*. Cluster analysis comparing all PL groupings identified sufficient dissimilarity between *gat2Δlpt1Δ* and *gat1Δlpt1Δ* to warrant placement in a separate group (Fig. 4A). This provided an initial indication that Gat1p has a greater preference for unsaturated acyl chains than Gat2p.
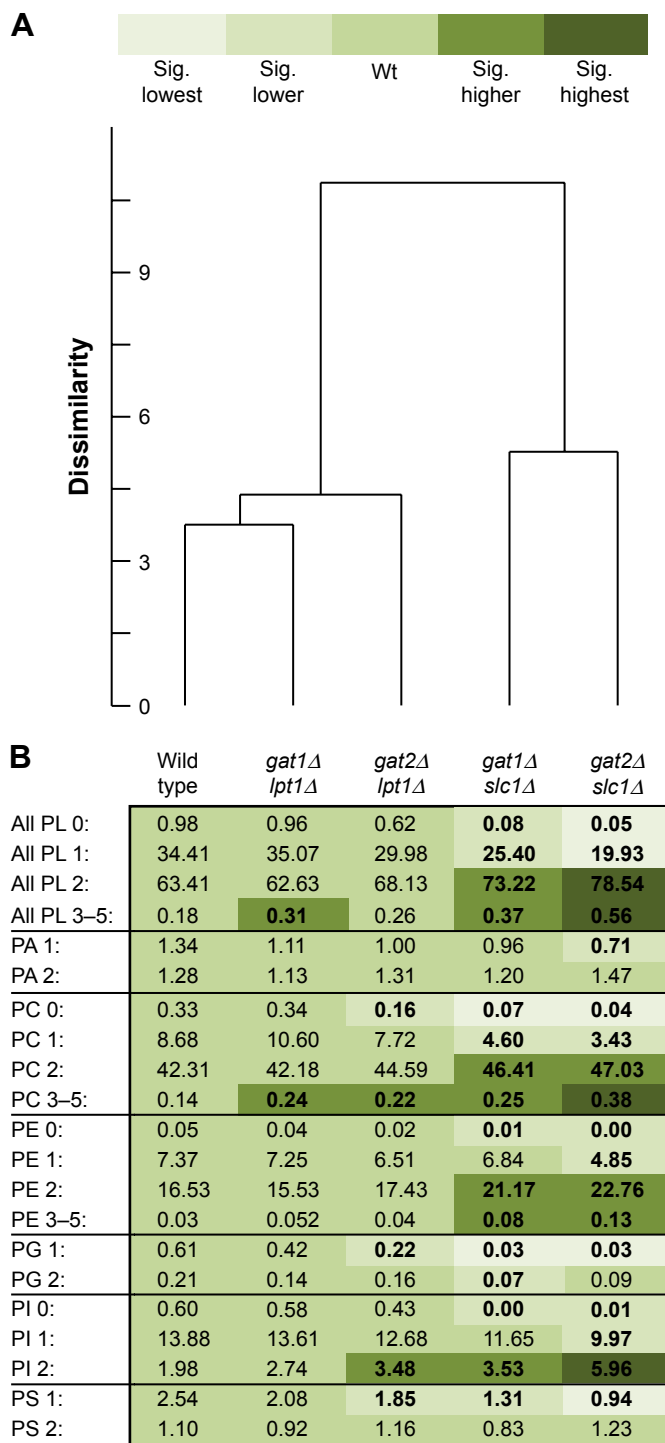
Leaving Gat2p as the main GPAT paired with Lpt1p in *gat1Δslc1Δ* strengthened the favoring of unsaturated acyl chain incorporation. Similar to others who found no PI 26:0 or 28:0 in *slc1Δ* strains,[16] almost no disaturated (:0) species of any length were found in *gat1Δslc1Δ*. This was striking in PI since the sn-1 position is routinely remodeled, mediated in part by *Psi1p*, which selectively incorporates saturated stearoyl chains.[17] Presuming that *Psi1p* activity is not affected in the mutants, the ability to synthesize PL with a saturated chain in the sn-2 position is nearly abrogated in *gat1Δslc1Δ*. This emphasizes the limited utilization of saturated acyl-CoA species by Lpt1p and indicates an absence of other acyltransferases that selectively incorporate saturated acyl chains into the sn-2 position of PI.

Even more skewed toward unsaturated acyl chains are the PL species in the *gat2Δslc1Δ* strains. The trend is observed in PA (Fig. 4B) and ripples through to the other head group species. This further suggests that Gat1p utilizes unsaturated acyl chains to a greater extent than Gat2p. Interestingly, the PL species with three to five double bonds, albeit at low concentrations, were most abundant in *gat2Δslc1Δ* strains. While *S. cerevisiae* only has the capability to introduce one double bond per acyl-CoA,[1] exogenous, polyunsaturated fatty acids, as may exist in undefined media such as YPD, can be readily incorporated.[8] This agrees with microsomal assays where polyunsaturated acyl-CoA species were incorporated into lysoPC by Lpt1p.[28,31] The clear decrease in disaturated and monounsaturated PL species and increase in diunsaturated species in both strains with *SLC1* deleted compared to the two strains with *LPT1* deleted, reflected by distinct clustering (Fig. 4A), suggests that in vivo Lpt1p utilizes unsaturated acyl chains to a greater extent than Slc1p.

Distribution of acyl chains in wild-type and mutant yeast: number of carbons. Since PL acyl chain length impacts interleaflet interactions within bilayers,[1] we also examined the influence of the respective GPATs and AGPATs on PL acyl

| | Sig. lowest | Sig. lower | Wt | Sig. higher | Sig. highest |

B	Wild type	*gat1Δ lpt1Δ*	*gat2Δ lpt1Δ*	*gat1Δ slc1Δ*	*gat2Δ slc1Δ*
All PL 0:	0.98	0.96	0.62	**0.08**	**0.05**
All PL 1:	34.41	35.07	29.98	**25.40**	**19.93**
All PL 2:	63.41	62.63	68.13	**73.22**	**78.54**
All PL 3–5:	0.18	**0.31**	0.26	**0.37**	**0.56**
PA 1:	1.34	1.11	1.00	0.96	**0.71**
PA 2:	1.28	1.13	1.31	1.20	1.47
PC 0:	0.33	0.34	**0.16**	**0.07**	**0.04**
PC 1:	8.68	10.60	7.72	**4.60**	**3.43**
PC 2:	42.31	42.18	44.59	**46.41**	**47.03**
PC 3–5:	0.14	**0.24**	**0.22**	**0.25**	**0.38**
PE 0:	0.05	0.04	0.02	**0.01**	**0.00**
PE 1:	7.37	7.25	6.51	6.84	**4.85**
PE 2:	16.53	15.53	17.43	**21.17**	**22.76**
PE 3–5:	0.03	0.052	0.04	**0.08**	**0.13**
PG 1:	0.61	0.42	**0.22**	**0.03**	**0.03**
PG 2:	0.21	0.14	0.16	**0.07**	0.09
PI 0:	0.60	0.58	0.43	**0.00**	**0.01**
PI 1:	13.88	13.61	12.68	11.65	**9.97**
PI 2:	1.98	2.74	**3.48**	**3.53**	**5.96**
PS 1:	2.54	2.08	**1.85**	**1.31**	**0.94**
PS 2:	1.10	0.92	1.16	0.83	1.23

Figure 4. Composition of phospholipids in wild-type and mutant strains: number of double bonds in acyl chains. Three strains of each genotype (two for *gat2Δslc1Δ*) were grown in YPD at 30°C until log phase on two different days ($n = 6$). Extracted lipids were analyzed by ESI-MS[2] and the abundance of each PL species expressed as the percent of total signal. Percentages were logit transformed and univariate statistical tests performed coupled with Tukey's post hoc test. (**A**) Hierarchical clustering was performed according to the PL distribution by number of double bonds.[44] (**B**) Percent composition of PL species presented in a heat map format. Significantly (sig.) higher or lower indicates difference compared to wild type ($p \leq 0.05$). Sig. highest or lowest indicates significant difference ($p \leq 0.05$) compared to values significantly higher or lower than wild type, respectively.

chain lengths. As with acyl chain distribution with regard to unsaturation, a gradation of phenotypes, reflected by clustering (Fig. 5A), was observed. Almost no differences were observed between wild-type and *gat1Δlpt1Δ* yeast. Almost every PL species was significantly higher or lower in *gat2Δslc1Δ* compared to wild type. Intermediate PL abundances were found in *gat2Δlpt1Δ* and *gat1Δslc1Δ* (Fig. 5A and B). One trend among the mutants, besides *gat1Δlpt1Δ*, was an increased abundance of PL with 32 and 36 carbons and fewer PL with 34 carbons. Since most yeast fatty acids have 16 or 18 carbons, the mutants have an increased ability to generate, regarding length, *homoacylated* PL and a decreased ability to make *heteroacylated* PL species compared to wild type. Since the AGPAT reaction dictates the second acyl chain that is paired with the initial acyl chain placed into lysoPA by GPAT, Slc1p and Lpt1p are the prime suspects for controlling acyl chain pairing. In a way, the situation resembles a genetic scenario where two alleles may be linked or inherited independently. Independent assortment (ie, lack of selective pairing) will allow the probability of each acyl chain, P(16:) and P(18:), to fit into a Hardy–Weinberg-like equation: $P(16:)^2 + 2P(16:)P(18:) + P(18:)^2 = 1$. Accordingly, our null hypothesis was that there was independent assortment (ie, nonselectivity) so that the sum of P(16:) and P(18:) would equal one.

To use this analogy and this hypothesis, some simplifying assumptions are required. Acyl chain populations will be limited to be C16 or C18 so that all 32: species have two 16 carbon chains (and not one 14 and one 18, for example) and only PL species with 32, 34, or 36 carbons will be analyzed. With those assumptions, the square root of the proportion of PL 32: species will equal the probability of a 16 carbon acyl chain being incorporated, P(16:), by either GPAT or AGPAT. Likewise, the square root of the proportion of PL 36: species will equal the probability of an 18 carbon chain being incorporated, P(18:). Using the data to derive these two probabilities allows for the proportion of PL 34: species to be predicted by 2P(16:)P(18:). If the proportion of PL 34: species predicted is the same as the observed, then independent assortment will be supported. However, if there are more PL 34: observed than predicted, then selective pairing with a bias toward heteroacylated PL will be supported. Conversely, if there are fewer PL 34: than predicted, then selective pairing with a bias toward homoacylated PL will be supported.

Using this analysis, the proportion of PL 34: observed almost exactly matches the expected for all PL and PL separated by head group in the *gat2Δslc1Δ* yeast (Table 2). Therefore, after Gat1p transfers the first acyl chain to form lysoPA, Lpt1p attaches the second acyl chain independent of the acyl chain in the sn-1 position. This is in stark contrast to the wild-type and *gat1Δlpt1Δ* strains, where the difference between the observed and expected probabilities ranges from 0.15 in PI to over 0.6 in PS (Table 2). Slc1p, therefore, likely does not have simple acyl-CoA substrate specificity. Instead, the efficiency with which an acyl-CoA is used depends on the

A

| Sig. lowest | Sig. lower | Wt | Sig. higher | Sig. highest |

B

	Wild type	*gat1Δ lpt1Δ*	*gat2Δ lpt1Δ*	*gat1Δ slc1Δ*	*gat2Δ slc1Δ*
All 26, 28:	1.94	1.93	1.45	**0.15**	**0.12**
All PL 30:	2.72	**3.34**	3.11	2.70	2.46
All PL 32:	33.18	33.17	35.13	**45.11**	**42.21**
All PL 34:	53.68	53.59	**49.14**	**42.48**	**42.37**
All PL 36:	6.88	6.25	**9.38**	7.53	**10.29**
All PL 38:	0.07	0.09	**0.13**	**0.31**	**0.42**
PA 32:	0.87	0.78	0.90	1.10	1.11
PA 34:	1.70	1.41	1.29	**0.99**	**0.90**
PA 36:	0.05	0.05	**0.12**	0.08	**0.17**
PC 26, 28:	1.26	1.26	0.94	**0.13**	**0.10**
PC 30:	1.89	2.41	1.94	**1.53**	**1.18**
PC 32:	20.26	20.87	21.45	**22.62**	20.10
PC 34:	24.69	25.63	23.90	**22.03**	23.36
PC 36:	3.03	2.76	**4.01**	**4.33**	**5.24**
PC 38:	0.06	**0.08**	**0.08**	**0.25**	**0.25**
PE 26, 28:	0.22	0.23	0.22	**0.02**	**0.02**
PE 30:	0.41	0.44	**0.61**	**0.78**	**0.80**
PE 32:	7.05	6.56	7.82	**14.09**	**13.95**
PE 34:	15.23	14.77	13.80	**11.80**	**10.45**
PE 36:	0.94	**0.71**	**1.36**	1.15	**2.09**
PE 38:	0.01	0.01	**0.02**	**0.03**	**0.05**
PG 32:	0.35	**0.26**	**0.13**	**0.02**	**0.03**
PG 34:	0.47	0.29	0.26	**0.08**	**0.09**
PI 26, 28:	0.46	0.44	0.30	**0.00**	**0.00**
PI 30:	0.40	0.47	0.51	0.34	0.41
PI 32:	3.81	3.98	3.94	**6.20**	5.87
PI 34:	8.89	9.26	8.02	**6.60**	**6.88**
PI 36:	2.82	2.70	**3.71**	**1.92**	2.53
PI 38:	0.00	0.00	**0.03**	**0.02**	**0.11**
PS 30:	0.03	0.02	**0.05**	**0.04**	**0.07**
PS 32:	0.85	0.71	0.88	1.07	1.15
PS 34:	2.70	2.23	**1.87**	**0.98**	**0.69**
PS 36:	0.05	**0.03**	**0.19**	0.05	**0.25**

Figure 5. Composition of phospholipids in wild-type and mutant strains: number of carbons in acyl chains. Yeast were cultured and analyzed as reported in Figure 4 except PL were grouped according to the number of carbons in the acyl chains.

Table 2. Proportion of PL 34: (heteroacylated) species in wild type and mutants: observed and predicted.

PL SPECIES	PROPORTION OF PL AS 34: SPECIES				
	WILD TYPE	*gat1Δlpt1Δ*	*gat2Δlpt1Δ*	*gat1Δslc1Δ*	*gat2Δslc1Δ*
All PL; observed	0.57 (0.01)	0.58 (0.02)	0.52 (0.01)	0.45 (0.01)	0.45 (0.01)
All PL; predicted	0.32 (0.00)	0.31 (0.01)	0.39 (0.01)	0.39 (0.01)	0.44 (0.01)
PA; observed	0.65 (0.02)	0.63 (0.02)	0.56 (0.02)	0.46 (0.01)	0.41 (0.02)
PA; predicted	0.16 (0.02)	0.18 (0.04)	0.28 (0.01)	0.27 (0.03)	0.40 (0.02)
PC; observed	0.52 (0.02)	0.52 (0.02)	0.48 (0.01)	0.45 (0.01)	0.48 (0.01)
PC; predicted	0.33 (0.01)	0.31 (0.01)	0.38 (0.01)	0.40 (0.01)	0.42 (0.01)
PE; observed	0.66 (0.02)	0.67 (0.01)	0.60 (0.01)	0.44 (0.01)	0.39 (0.01)
PE; predicted	0.22 (0.01)	0.20 (0.01)	0.28 (0.01)	0.30 (0.01)	0.41 (0.01)
PI; observed	0.57 (0.01)	0.58 (0.01)	0.51 (0.01)	0.50 (0.01)	0.45 (0.01)
PI; predicted	0.42 (0.00)	0.41 (0.01)	0.49 (0.01)	0.47 (0.01)	0.50 (0.01)
PS; observed	0.75 (0.02)	0.75 (0.02)	0.64 (0.02)	0.46 (0.05)	0.33 (0.08)
PS; predicted	0.11 (0.02)	0.07 (0.05)	0.28 (0.02)	0.22 (0.03)	0.51 (0.06)

Notes: The probability of a 16 carbon acyl chain, P(16:), or an 18 carbon acyl chain, P(18:), in all PL or in each PL species (by head group) was calculated as the square root of the proportion of the 32: and 36: species, respectively. Predicted proportion of PL 34: = 2P(16:)P(18:). Standard deviation is in parentheses.

acyl chain in the lysoPA substrate. This explains acyl chain pairing. Since the *gat2Δlpt1Δ* yeast have lower proportions of PL 34: species than wild type (Table 2), Gat2p is necessary along with Slc1p for maximal heteroacylation.

Interestingly, the expected and observed 34: abundances in PA are more different than in all PL. To account for this, the enzymes that utilize PA and subsequent intermediates in the pathway may have substrate specificity regarding acyl chain composition and thus influence the acyl chain compositions associated with different head groups. Previous work supports such specificity regarding PE methylation.[11] In addition to selective utilization, remodeling of PL after head group addition may also account for the distinctly different acyl chain composition of PA and other PL. However, when only one main GPAT and AGPAT are expressed, the acyltransferases used in de novo synthesis and remodeling are, with the exception of Psi1p, likely the same. These data provide further evidence that in the growth conditions used, Gat2p and Slc1p are the isoenzymes that primarily influence acyl chain distribution in PL.

Also clear from Figure 5 is the repeated observation that strains expressing Gat1p (ie, *gat2Δ*) have a greater abundance of PL 36: species than strains expressing Gat2p, regardless of the accompanying AGPAT. This is consistent with Gat2p, relative to Gat1p, preferentially using acyl-CoA species with 16 carbons. Overexpression of *GAT2* followed by ESI-MS[2] and in vitro GPAT assays support the same conclusion.[14,19]

Distribution of acyl chains in wild-type and mutant yeast: head groups. Coinciding with acyl chain pairing being particularly evident in PE and PS (Table 2) was the differing abundance of PE and PS among the genotypes (Fig. 6B). Yeast with *SLC1* deleted contained an increased proportion of PE and decreased proportions of PS and PG. One explanation

is that the atypical arrangement of acyl chains in PS provided improved substrates for phosphatidylserine decarboxylase, Psd1p, leading to accelerated PS consumption to form PE. Atypical acyl chain arrangements may cause decreased PE
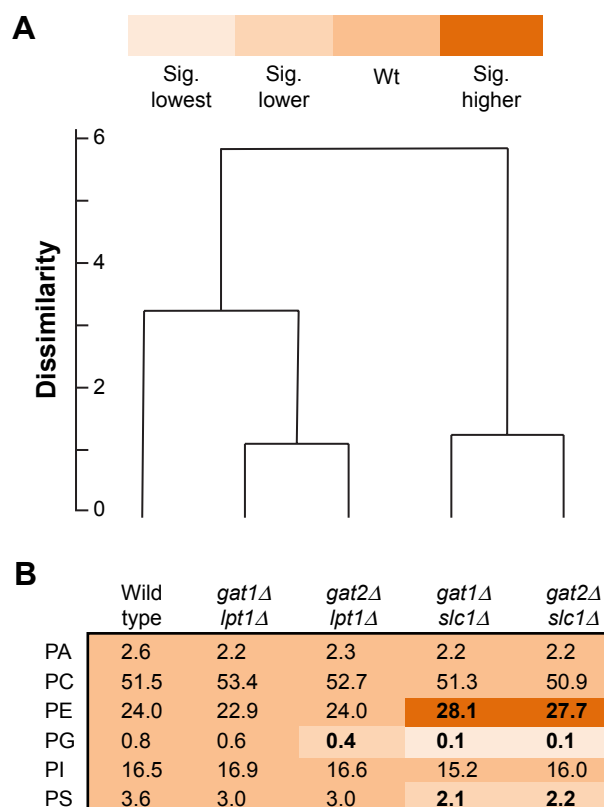
Figure 6. Composition of phospholipids in wild-type and mutant strains: head groups. Yeast were cultured and analyzed as reported in Figure 4 except PL were grouped according to head group.
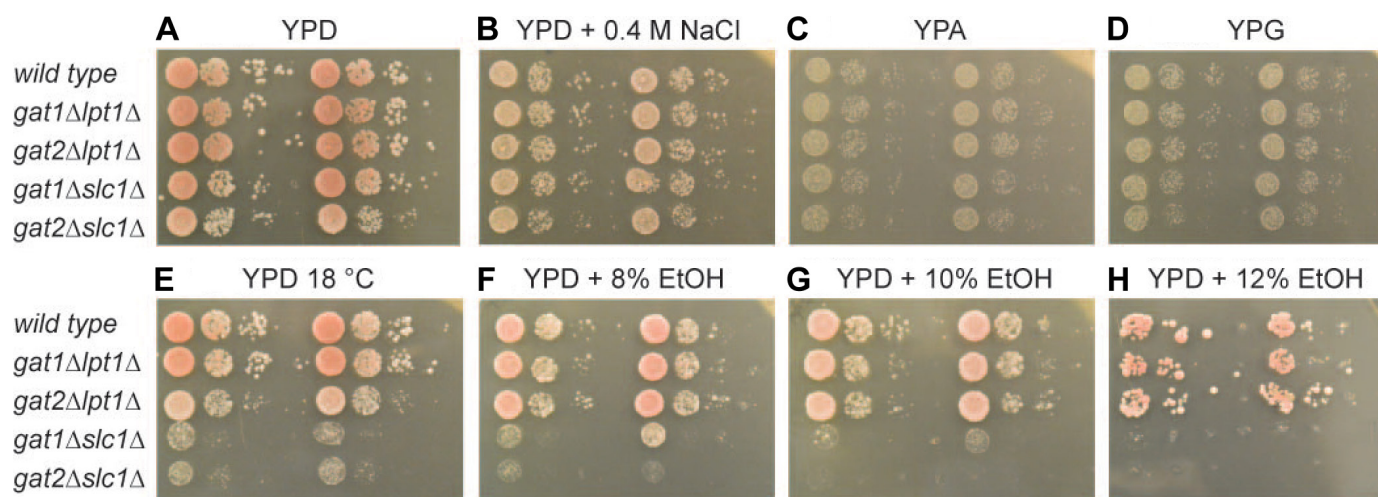
Figure 7. Membrane-related growth phenotypes in compound deletion mutants. Two strains of each genotype were cultured in YPD into log phase. Serial dilutions resulted in 4,000, 400, 40, and 4 cells being applied to sequential spots on agar plates. Incubation occurred for (**A–D**) 26 hours, (**E**) 55 hours, (**F**) 78 hours, (**G**) 107 hours, and (**H**) 185 hours.

methylation by Cho2p and Opi3p. Decreased abundance of PS and PG may also indicate reduced CDP-DAG production with preferential utilization for PI synthesis (Fig. 1). How PA produced by Lpt1p is partitioned differently than PA produced by Slc1p remains to be determined.

Assessment of growth phenotypes in compound deletion mutant strains. Given the continuum of changes in PL composition caused by the compound deletion mutant genotypes, we began to examine how these changes affect cellular function. Since growth and division is a comprehensive metric of cellular function, the ability of the mutant strains to grow, especially in environments that may strain membrane function, was measured (Fig. 7). Although growth on YPD solid media at 30°C was intended as a control (Fig. 7A), *gat2Δslc1Δ* strains showed a subtle reduction of colony abundance in the second dilution. Further examination showed that in liquid YPD at 30°C, *gat2Δslc1Δ* strains had a mean doubling time of 128 minutes, significantly longer ($P < 0.001$) than the 108 minutes of normal strains. The other mutants had doubling times similar to wild type (data not shown). Light microscopy of *gat2Δslc1Δ* cultures in late log phase did not detect any morphological phenotype (data not shown). Previously, *gat1Δ* and *gat2Δ* cultured in rich media with galactose displayed spherical and elongated phenotypes, respectively.[24]

Hyperosmotic stress (Fig. 7B) and provision of nonfermentable carbon sources that require oxidative catabolism (Fig. 7C and D) did not provide a detectable challenge to any of the mutants. This was unexpected since GPAT activity increased three-fold upon culturing in a nonfermentable carbon source.[46] Temperature did have an effect as *gat1Δslc1Δ* and *gat2Δslc1Δ* strains showed fewer colonies in all dilutions at 18.5°C (Fig. 7E). A modest, slow-growth phenotype in *gat2Δlpt1Δ* was also observed in the third dilution at 18.5°C. Since all three of those mutant genotypes impacted a variety

of PL species, a direct association of a PL change with cool temperature intolerance cannot be made. However, given the trend of more unsaturated and fewer saturated acyl chains in these strains, the phenotype was unexpected since yeast upregulate the acyl-CoA desaturase *OLE1* when shifted to 10°C.[47] However, a subtle increase in saturated fatty acid content occurs in yeast grown at 15°C versus 30°C.[48]

Growth in ethanol was also assayed (Fig. 7F–H) since ethanol is known to intercalate into PL bilayers and cause membrane thinning.[49] Membranes enriched with PL containing oleoyl groups are resistant to such damage.[50] Dextrose was included in the media so that ethanol utilization as a carbon source was not required. Both strains with *slc1Δ* showed a distinct, lower growth phenotype (eg, no cells at second dilution) at all concentrations of ethanol provided. In 10% ethanol, *gat1Δ–slc1Δ* showed a reproducible, limited ability to grow at the first dilution, while the *gat2Δslc1Δ* strains were essentially inviable. Previously, growth in YP with 2% ethanol increased abundance of unsaturated acyl chains.[51] The data presented here suggest that yeast exposed to higher levels of ethanol while undergoing fermentation do not benefit from increased abundance of unsaturated acyl chains in PL. Perhaps the increased abundance of PE, a nonbilayer PL, in both *slc1Δ* mutants renders the membranes more susceptible to ethanol-mediated disruption.

Discussion

Previously, the acyltransferases involved in PL synthesis and remodeling have mostly been analyzed in cell fractions using an assortment of in vitro conditions. These conditions have largely been limited to a subset of possible substrate combinations (ie, acyl-CoA and acyl-acceptor) at single concentrations. The present study is the first to make a comprehensive, in vivo assessment of the substrate utilization of multiple GPATs and AGPATs in any organism.

One particular benefit of in vivo studies is that they may ascertain the relative physiological contribution of potentially redundant isoenzymes. Certainly, environmental conditions may influence the relative contributions of the isoenzymes. With the caveat that common laboratory growth conditions were used, our data uniquely support that Gat2p is the GPAT that primarily influences PL composition in *S. cerevisiae*. This predominance of Gat2p conflicts with in vitro GPAT assays using palmitoyl-CoA, which show a greater reduction in activity in *gat1Δ* lysates than *gat2Δ* lysates.[24] Western blots showing similar expression levels of genomically epitope-tagged Gat1p and Gat2p suggest that higher expression of Gat2p is not a likely reason for its primary role.[24]

Our data also support that Gat2p promotes greater incorporation of saturated acyl chains than Gat1p. This is consistent with in vitro assays of GPAT activity in *gat1Δ* and *gat2Δ* strains,[19] gas chromatography analysis of cellular fatty acids in *gat1Δ* strains,[52] and ESI-MS[2] analysis of lipids from cells overexpressing *GAT1*.[14,23] However, the acyl chain preference of Gat1p versus Gat2p was not evident with pulse labeling as the total incorporation of palmitic acid and oleic acid was similar among the mutants. This may be due to rapid desaturation of palmitoyl-CoA.

Deleting either GPAT with *SLC1* had a more profound influence on cellular PL composition than the paired deletion of either GPAT with *LPT1*. This allows the novel conclusion that Slc1p is the AGPAT that primarily influences PL composition in *S. cerevisiae*. Since Slc1p has been shown to poorly utilize lysoPC and lysoPE and since deletion of *LPT1* dramatically reduces the esterification of all 1-acyl-2-hydroxy lysoPL besides lysoPA,[15,28,29,31,36] these data support that in rich media at 30°C, de novo synthesis predominantly dictates PL acyl chain composition at the sn-2 position. Confirmatory was the finding that Lpt1p has a greater likelihood of incorporating unsaturated acyl chains. In vitro assays with *slc1Δ* lysates and *lpt1Δ* lysates,[28,30–32,36] gas chromatography of cellular fatty acids in wild-type and *slc1Δ* strains,[52] and ESI-MS[2] analysis of *slc1Δ* and *lpt1Δ* strains all support that Slc1p has a mild to distinct preference for saturated acyl-CoA species, while Lpt1p much more efficiently utilizes unsaturated acyl-CoAs.[15,16]

While the different substrate specificities of the four acyltransferases allow for an array of PA species to be stochastically produced, these specificities are insufficient to account for the preponderance of cellular PL species with two acyl chains containing 34 carbons. Uniquely, the current study supports an explanation. Slc1p has substrate specificity that promotes discrete acyl chain pairing. 16 carbon acyl-CoAs are preferentially joined with lysoPA species with an 18 carbon acyl chain, and 18 carbon acyl-CoAs are preferentially joined with lysoPA species with 16 carbon acyl chains. Aside from phospholipases, there are few enzymes that have a characterized preference for glycerolipid substrates with specific acyl chain composition. Human DAG kinase ε utilized DAG species with an sn-2 arachidonyl chain with about 10-fold

greater velocity than when dioleoylglycerol was supplied.[53] This may streamline PI remodeling in the PI signaling cycle.

Why a mechanism exists to favor 34 carbon, heteroacylated PL synthesis is another question. In PL, the sn-1 acyl chain often extends further into bilayers than the sn-2. Having a 16 carbon acyl chain at sn-1, promoted by Gat2p, and an 18 carbon acyl chain at sn-2, promoted by Slc1p, provides more uniform extension of the terminal methyl groups and facilitates interleaflet overlap and coupling.[1] Also, oleoyl chains in model PL bilayers showed greater flexibility to bend back toward the membrane water interface when paired with a shorter, saturated acyl chain.[1] Perhaps the formation of heteroacylated PL explains why jointly supplying palmitic acid and oleic acid to fatty acid synthesis deficient yeast allowed for normal mitochondrial function and cytochrome c oxidase activity.[54] Preferential formation of heteroacylated PL also limits the production of homoacylated PL species. PA with 32 carbon acyl chains is particularly able to bind the Opi1p transcription factor.[7] Gat1p and Lpt1p may be specialized to shift the PL composition toward more homoacylated and unsaturated acyl chains as needed. Our data also support that mechanisms do not exist for *OLE1* to be downregulated enough to limit the overproduction of unsaturated acyl chain enriched PL as occurs in *gat2Δslc1Δ* yeast. Determining how the substrate specificities of the yeast GPATs and AGPATs influence the composition of DAG and how DAG composition influences the acyltransferases that esterify it to produce TAG will further elucidate how yeast allocate acyl chains.

In addition to providing insight into acyl chain distribution, the compound deletion mutants, with a continuum of hardwired PL profiles regarding acyl chain length and number of double bonds, provide a background in which to study the impact of PL composition on cellular processes.

Acknowledgments

Author Contributions

Conceived and designed the experiments: PO. Analyzed the data: PO and KP. Wrote the first draft of the manuscript: PO. Contributed to the writing of the manuscript: PO and KP. Agreed with manuscript results and conclusions: PO and KP. Jointly developed the structure and arguments for the paper: PO and KP. Made critical revisions and approved the final version: PO and KP. All the authors reviewed and approved the final manuscript.

REFERENCES

1. Capponi S, Freites JA, Tobias DJ, White SH. Interleaflet mixing and coupling in liquid-disordered phospholipid bilayers. *Biochim Biophys Acta*. 2016;1858: 354–362.

2. Domanska MK, Kiessling V, Tamm LK. Docking and fast fusion of synapto-brevin vesicles depends on the lipid compositions of the vesicle and the acceptor SNARE complex-containing target membrane. *Biophys J*. 2010;99:2936–2946.

3. Ramadurai S, Duurkens R, Krasnikov VV, Poolman B. Lateral diffusion of membrane proteins: consequences of hydrophobic mismatch and lipid composition. *Biophys J*. 2010;99:1482–1489.

4. Vitrac H, MacLean DM, Jayaraman V, Bogdanov M, Dowhan W. Dynamic membrane protein topological switching upon changes in phospholipid environment. *Proc Natl Acad Sci U S A*. 2015;112:13874–13879.

5. Sugano K, Hamada H, Machida M, Ushio H. High throughput prediction of oral absorption: improvement of the composition of the lipid solution used in parallel artificial membrane permeation assay. *J Biomol Screen*. 2001;6:189–196.

6. Chakravarthy MV, Lodhi IJ, Yin L, et al. Identification of a physiologically relevant endogenous ligand for PPARα in liver. *Cell*. 2009;138:476–488.

7. Hofbauer HF, Schopf FH, Schleifer H, et al. Regulation of gene expression through a transcriptional repressor that senses acyl-chain length in membrane phospholipids. *Dev Cell*. 2014;29:729–739.

8. Stukey JE, McDonough VM, Martin CE. Isolation and characterization of *OLE1*, a gene affecting fatty acid desaturation from *Saccharomyces cerevisiae*. *J Biol Chem*. 1989;264:16537–16544.

9. Wagner S, Paltauf F. Generation of glycerophospholipid molecular species in the yeast *Saccharomyces cerevisiae*. Fatty acid pattern of phospholipid classes and selective acyl turnover at sn-1 and sn-2 positions. *Yeast*. 1994;10:1429–1437.

10. Ejsing CS, Sampaio JL, Surendranath V, et al. Global analysis of the yeast lipidome by quantitative shotgun mass spectrometry. *Proc Natl Acad Sci U S A*. 2009;106:2136–2141.

11. Boumann HA, Damen MJ, Versluis C, Heck AJ, de Kruijff B, de Kroon AI. The two biosynthetic routes leading to phosphatidylcholine in yeast produce different sets of molecular species. Evidence for lipid remodeling. *Biochemistry*. 2003; 42:3054–3059.

12. Schneiter R, Brügger B, Sandhoff R, et al. Electrospray ionization tandem mass spectrometry (ESI-MS/MS) analysis of the lipid molecular species composition of yeast subcellular membranes reveals acyl chain-based sorting/remodeling of distinct molecular species en route to the plasma membrane. *J Cell Biol*. 1999;146:741–754.

13. Henderson CM, Zeno WF, Lerno LA, Longo ML, Block DE. Fermentation temperature modulates phosphatidylethanolamine and phosphatidylinositol levels in the cell membrane of *Saccharomyces cerevisiae*. *Appl Environ Microbiol*. 2013;9:5345–5356.

14. De Smet CH, Vittone E, Scherer M, et al. The yeast acyltransferase Sct1p regulates fatty acid desaturation by competing with the desaturase Ole1p. *Mol Biol Cell*. 2012;23:1146–1156.

15. Benghezal M, Roubaty C, Veepuri V, Knudsen J, Conzelmann A. *SLC1* and *SLC4* encode partially redundant acyl-coenzyme A 1-acylglycerol-3-phosphate O acyltransferases of budding yeast. *J Biol Chem*. 2007;282:30845–30855.

16. Guan XL, Wenk MR. Mass spectrometry-based profiling of phospholipids and sphingolipids in extracts from *Saccharomyces cerevisiae*. *Yeast*. 2006;23:465–477.

17. Le Guedard M, Bessoule JJ, Boyer V, et al. *PSI1* is responsible for the stearic acid enrichment that is characteristic of phosphatidylinositol in yeast. *FEBS J*. 2009;276:6412–6424.

18. Boumann HA, Gubbens J, Koorengevel MC, et al. Depletion of phosphatidylcholine in yeast induces shortening and increased saturation of the lipid acyl chains: evidence for regulation of intrinsic membrane curvature in a eukaryote. *Mol Biol Cell*. 2006;17:1006–1017.

19. Zheng Z, Zou J. The initial step of the glycerolipid pathway: identification of glycerol 3-phosphate/dihydroxyacetone phosphate dual substrate acyltransferases in *Saccharomyces cerevisiae*. *J Biol Chem*. 2001;276:41710–41716.

20. Lockshon D, Surface LE, Kerr EO, Kaeberlein M, Kennedy BK. The sensitivity of yeast mutants to oleic acid implicates the peroxisome and other processes in membrane function. *Genetics*. 2007;175:77–91.

21. Marr N, Foglia J, Terebiznik M, Athenstaedt K, Zaremberg V. Controlling lipid fluxes at glycerol-3-phosphate acyltransferase step in yeast: unique contribution of Gat1p to oleic acid-induced lipid particle formation. *J Biol Chem*. 2012;287: 10251–10264.

22. Zaremberg V, McMaster CR. Differential partitioning of lipids metabolized by separate yeast glycerol-3-phosphate acyltransferases reveals that phospholipase D generation of phosphatidic acid mediates sensitivity to choline-containing lysolipids and drugs. *J Biol Chem*. 2002;277:39035–39044.

23. De Smet CH, Cox R, Brouwers JF, de Kroon AI. Yeast cells accumulate excess endogenous palmitate in phosphatidylcholine by acyl chain remodeling involving the phospholipase B Plb1p. *Biochim Biophys Acta*. 2013;1831:1167–1176.

24. Bratschi MW, Burrowes DP, Kulaga A, et al. Glycerol-3-phosphate acyltransferases Gat1p and Gat2p are microsomal phosphoproteins with differential contributions to polarized cell growth. *Eukaryot Cell*. 2009;8:1184–1196.

25. Loewen CJR, Gaspar ML, Jesch SA, et al. Phospholipid metabolism regulated by a transcription factor sensing phosphatidic acid. *Science*. 2004;304:1644–1647.

26. Vögtle FN, Keller M, Taskin AA, et al. The fusogenic lipid phosphatidic acid promotes the biogenesis of mitochondrial outer membrane protein Ugo1. *J Cell Biol*. 2015;210:951–960.

27. Nagiec MM, Wells GB, Lester RL, Dickson RC. A suppressor gene that enables *Saccharomyces cerevisiae* to grow without making sphingolipids encodes a protein that resembles an *Escherichia coli* fatty acyltransferase. *J Biol Chem*. 1993;268:22156–22163.

28. Jain S, Stanford N, Bhagwat N, et al. Identification of a novel lysophospholipid acyltransferase in *Saccharomyces cerevisiae*. *J Biol Chem*. 2007;282:30562–30569.

29. Riekhof WR, Wu J, Jones JL, Voelker DR. Identification and characterization of the major lysophosphatidylethanolamine acyltransferase in *Saccharomyces cerevisiae*. *J Biol Chem*. 2007;282:28344–28352.

30. Chen Q, Kazachkov M, Zheng Z, Zou J. The yeast acylglycerol acyltransferase *LCA1* is a key component of Lands cycle for phosphatidylcholine turnover. *FEBS Lett*. 2007;581:5511–5516.

31. Tamaki H, Shimada A, Ito Y, et al. LPT1 encodes a membrane-bound O-acyltransferase involved in the acylation of lysophospholipids in the yeast *Saccharomyces cerevisiae*. *J Biol Chem*. 2007;282:34288–34298.

32. Stahl U, Stalberg K, Stymne S, Ronne H. A family of eukaryotic lysophospholipid acyltransferases with broad specificity. *FEBS Lett*. 2008;582:305–309.

33. Ghosh AK, Ramakrishnan G, Rajasekharan R. YLR099C (*ICT1*) encodes a soluble acyl-CoA-dependent lysophosphatidic acid acyltransferase responsible for enhanced phospholipid synthesis on organic solvent stress in *Saccharomyces cerevisiae*. *J Biol Chem*. 2008;283:9768–9775.

34. Ayciriex S, Le Guédard M, Camougrand N, et al. YPR139c/*LOA1* encodes a novel lysophosphatidic acid acyltransferase associated with lipid droplets and involved in TAG homeostasis. *Mol Biol Cell*. 2012;23:233–246.

35. Shui G, Guan XL, Gopalakrishnan P, et al. Characterization of substrate preference for Slc1p and Cst26p in *Saccharomyces cerevisiae* using lipidomic approaches and an LPAAT activity assay. *PLoS One*. 2010;5:e11956.

36. Riekhof WR, Wu J, Gijon MA, Zarini S, Murphy RC, Voelker DR. Lysophosphatidylcholine metabolism in *Saccharomyces cerevisiae*; the role of P-type ATPases in transport and a broad specificity acyltransferase in acylation. *J Biol Chem*. 2007; 282:36853–36861.

37. Tanaka K, Fukuda R, Ono Y, et al. Incorporation and remodeling of extracellular phosphatidylcholine with short acyl residues in *Saccharomyces cerevisiae*. *Biochim Biophys Acta*. 2008;1781:391–399.

38. Ayyash M, Algahmi A, Gillespie J, Oelkers P. Characterization of a lysophospholipid acyltransferase involved in membrane remodeling in *Candida albicans*. *Biochim Biophys Acta*. 2014;184:505–513.

39. Thomas BJ, Rothstein R. Elevated recombination rates in transcriptionally active DNA. *Cell*. 1989;56:619–630.

40. Rothstein R. Targeting, disruption, replacement, and allele rescue: integrative DNA transformation in yeast. *Methods Enzymol*. 1991;194:281–301.

41. Oelkers P, Cromley D, Padamsee M, Billheimer JT, Sturley SL. The *DGA1* gene determines a second triacylglycerol synthetic pathway in yeast. *J Biol Chem*. 2002; 277:8877–8881.

42. Lattif AA, Mukherjee PK, Chandra J, et al. Lipidomics of *Candida albicans* biofilms reveals phase-dependent production of phospholipid molecular classes and role for lipid rafts in biofilm formation. *Microbiology*. 2011;157:3232–3242.

43. Aitchison J. The statistical analysis of compositional data. *J R Stat Soc B*. 1982;44: 139–177.

44. Anderberg MR. *Cluster Analysis for Applications*. New York: Academic Press; 1973.

45. Færgeman NJ, Black PN, Zhao XD, Knudsen J, DiRusso CC. The Acyl-CoA synthetases encoded within *FAA1* and *FAA4* in *Saccharomyces cerevisiae* function as components of the fatty acid transport system linking import, activation, and intracellular utilization. *J Biol Chem*. 2001;276:37051–37059.

46. Minskoff SA, Racenis PV, Granger J, Larkins L, Hajra AK, Greenberg ML. Regulation of phosphatidic acid biosynthetic enzymes in *Saccharomyces cerevisiae*. *J Lipid Res*. 1994;35:2254–2262.

47. Nakagawa Y, Sakumoto N, Kaneko Y, Harashima S. Mga2p is a putative sensor for low temperature and oxygen to induce *OLE1* transcription in *Saccharomyces cerevisiae*. *Biochem Biophys Res Commun*. 2002;291:707–713.

48. Martin CE, Oh CS, Jiang Y. Regulation of long chain unsaturated fatty acid synthesis in yeast. *Biochim Biophys Acta*. 2007;1771:271–285.

49. Ly HV, Longo ML. The influence of short-chain alcohols on interfacial tension, mechanical properties, area/molecule, and permeability of fluid lipid bilayers. *Biophys J*. 2004;87:1013–1033.

50. Vanegas JM, Contreras MF, Faller R, Longo ML. Role of unsaturated lipid and ergosterol in ethanol tolerance of model yeast biomembranes. *Biophys J*. 2012; 102:507–516.

51. Tuller G, Nemec T, Hrastnik C, Daum G. Lipid composition of subcellular membranes of an FY1679-derived haploid yeast wild-type strain grown on different carbon sources. *Yeast*. 1999;15:1555–1564.

52. Athenstaedt K, Daum G. Biosynthesis of phosphatidic acid in lipid particles and endoplasmic reticulum of *Saccharomyces cerevisiae*. *J Bacteriol*. 1997;179:7611–7616.

53. Lung M, Shulga YV, Ivanova PT, et al. Diacylglycerol kinase epsilon is selective for both acyl chains of phosphatidic acid or diacylglycerol. *J Biol Chem*. 2009;284: 31062–31073.

54. Trivedi A, Fantin DJ, Tustanoff ER. Role of phospholipid fatty acids on the kinetics of high and low affinity sites of cytochrome c oxidase. *Biochem Cell Biol*. 1986;64:1195–1210.